

Distributed Switching Model Predictive Control Meets Koopman Operator for Dynamic Obstacle Avoidance

Ali Azarbahram * Chrystian Pool Yuca Huanca **
 Gian Paolo Incremona ** Patrizio Colaneri **

* *The Department of Electrical Engineering, Chalmers University of Technology, Gothenburg, 412 96, Sweden. (e-mail: ali.azarbahram@chalmers.se).*

** *The Dipartimento di Elettronica, Informazione e Bioingegneria, Politecnico di Milano, 20133 Milan, Italy. (e-mails: {chrystianpool.yuca, gianpaolo.incremona, and patrizio.colaneri}@polimi.it).*

Abstract: This paper introduces a Koopman-enhanced distributed switched model predictive control (SMPC) framework for safe and scalable navigation of quadrotor unmanned aerial vehicles (UAVs) in dynamic environments with moving obstacles. The proposed method integrates switched motion modes and data-driven prediction to enable real-time, collision-free coordination. A localized Koopman operator approximates nonlinear obstacle dynamics as linear models based on online measurements, enabling accurate trajectory forecasting. These predictions are embedded into a distributed SMPC structure, where each UAV makes autonomous decisions using local and cluster-based information. This computationally efficient architecture is particularly promising for applications in surface transportation, including coordinated vehicle flows, shared infrastructure with pedestrians or cyclists, and urban UAV traffic. Simulation results demonstrate reliable formation control and real-time obstacle avoidance, highlighting the framework's broad relevance for intelligent and cooperative mobility systems.

Keywords: Koopman operator, switched model predictive control, distributed control, dynamic obstacle avoidance, quadrotor UAVs.

1. INTRODUCTION

Cooperative unmanned aerial vehicle (UAV) navigation is increasingly vital in intelligent mobility systems, where safe interaction with other vehicles, infrastructure, and dynamic road users is paramount (Scherer et al., 2008). Multi-UAV coordination enhances situational awareness and coverage (Michael et al., 2011), but introduces safety and scalability challenges (Ponda et al., 2010; Zhou and Schwager, 2015). However, trajectory planning under actuator and collision constraints must remain computationally feasible for real-time deployment (Saccani et al., 2022; Tang and Kumar, 2018). Model predictive control (MPC) is widely used for such tasks (Mayne et al., 2005), while onboard sensing or direct avoidance is often required in partially unknown environments (Hrabar, 2011; Liu et al., 2017).

MPC's predictive and constraint-handling capabilities make it attractive for real-time control (Garcia et al., 1989; Kouvaritakis and Cannon, 2016), with switched MPC providing further efficiency by restricting the control to a predefined set of motion primitives (Bemporad and Morari, 1999; Huanca et al., 2023). These features align well with the challenges of urban UAV navigation operating in proximity to infrastructure or pedestrians.

Obstacle avoidance in dynamic environments demands both rapid response and reliable motion forecasting. Recent MPC-based methods have incorporated probabilistic and learning-based models for obstacle behavior (Li et al., 2023; Olcay et al., 2024; Wei et al., 2022). Despite this progress, few efforts address online modeling of unknown dynamics for embedded control. This motivates the use of the Koopman operator, which linearly embeds nonlinear systems into higher-dimensional spaces, enabling efficient data-driven prediction (Williams et al., 2015).

The Koopman operator has emerged as a powerful tool for bridging nonlinear dynamics and linear control frameworks. A comprehensive treatment of its theoretical underpinnings and relevance to systems and control is provided in (Mauroy et al., 2020), outlining its use in estimation, observability, and feedback design. The approach is utilized for controlled dynamical systems in (Korda and Mezić, 2018), where data-driven linear predictors are constructed in lifted spaces, enabling integration into efficient MPC schemes. The broader utility of the Koopman framework in forecasting, system identification, and controller synthesis is also surveyed in (Mezić, 2021). Koopman-based models have thus found success in motion planning (Gutow and Rogers, 2020), object tracking (Comas et al., 2021), robust control (Zhang et al., 2022), and mobility applications (Manzoor et al., 2023).

¹ This work has been supported by the Italian Ministry of Enterprises and Made in Italy in the framework of the project 4DDS (4D Drone Swarms) under grant no. F/310097/01-04/X56.

Building upon the earlier work (Bueno et al., 2025), which first introduced the use of the Koopman operator for modeling and predicting unknown moving obstacles in single-agent UAV navigation, this paper advances the concept to a multi-agent cooperative setting with distributed and switched predictive control. The proposed framework unifies Koopman-based data-driven forecasting with distributed switching MPC (SMPC), enabling real-time, decentralized, and collision-free coordination among multiple UAVs in dynamic environments with moving or fixed obstacles. The contributions are: i) a distributed SMPC framework with flexible motion modes and clustering, scalable to large multi-vehicle networks and ii) a Koopman-based obstacle prediction model embedded in SMPC via linear constraints, enabling safety by avoiding dynamic agents and obstacles in real time.

The remainder of the paper is structured as follows. Section 2 presents the problem formulation and preliminaries. Section 3 details the proposed method. Section 4 illustrates simulation results, and Section 5 concludes the paper with the proposal overview and suggests future directions.

2. PRELIMINARIES AND PROBLEM STATEMENT

This section details the quadrotor model, its reformulation into the switching framework with the corresponding discrete representation, and the problem statement.

2.1 Quadrotor UAV

This work considers a general UAV kinematic model suitable for various robotic platforms, assuming that embedded control loops handle the actuator dynamics. A local replanner is also assumed to ensure smooth velocity and acceleration references, including those from switched controllers (e.g., (Oleynikova et al., 2016)). Let $O_W - X_W Y_W Z_W$ denote the fixed world frame and $O_B - X_B Y_B Z_B$ the body frame attached to each UAV. Using Euler's equations, the absolute position and orientation vector $\bar{p} = [p \ \phi \ \theta \ \psi]^\top$, with $p = [p_x \ p_y \ p_z]^\top$, evolves based on the body velocity vector $v = [v_u \ v_v \ v_w \ w_p \ w_q \ w_r]^\top$ as

$$\dot{\bar{p}} = Rv, \quad (1)$$

where $R = \text{diag}(R_v, R_w)$ is block diagonal with:

$$R_v = \begin{bmatrix} c(\theta)c(\psi) & s(\phi)s(\theta)c(\psi)-c(\theta)s(\psi) & c(\phi)s(\theta)c(\psi)+s(\theta)s(\psi) \\ c(\theta)s(\psi) & s(\phi)s(\theta)s(\psi)+c(\theta)c(\psi) & c(\phi)s(\theta)s(\psi)-s(\theta)c(\psi) \\ -s(\theta) & s(\phi)c(\theta) & c(\phi)c(\theta) \end{bmatrix},$$

$$R_w = \begin{bmatrix} 1 & s(\phi)\tan(\theta) & c(\phi)\tan(\theta) \\ 0 & c(\phi) & -s(\phi) \\ 0 & s(\phi)c(\theta)^{-1} & c(\phi)c(\theta)^{-1} \end{bmatrix}.$$

Here, $c(\cdot)$ and $s(\cdot)$ denote $\cos(\cdot)$ and $\sin(\cdot)$. For clarity, we use the general continuous-time form of the kinematics in (1), where the absolute UAV pose \bar{p} is the state x and the body velocity v is the input u :

$$\dot{x} = f(x, u), \quad x(0) = x_0. \quad (2)$$

2.2 Switched UAV model

Switched systems offer a practical approach for large-scale distributed networks by reducing dynamics complexity through a finite set of motion modes (Huanca et al., 2023).

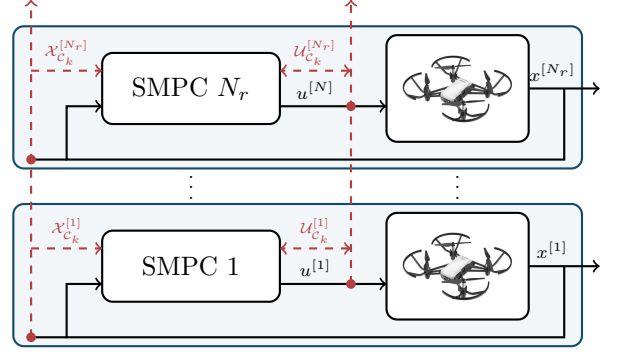


Fig. 1. Sequential distributed SMPC scheme.

We recast (2) into this framework. Consider N_r identical quadrotors indexed by $\mathcal{N} := \{i \mid i = 1, \dots, N_r\}$. Each UAV $[i]$ operates under a mode $\sigma^{[i]} \in \mathcal{M} := \{1, \dots, m\}$, governed by the control input $u^{[i]}(\sigma^{[i]}) \in \mathcal{U}_{\text{sw}}$, \mathcal{U}_{sw} being a predefined set of velocity vectors:

$$u^{[i]}(\sigma^{[i]}) = \begin{cases} 0_{6 \times 1}, & \sigma^{[i]} = 1 \\ \bar{v}e_{\sigma^{[i]}-1}, & \sigma^{[i]} = 2, 3, 4 \\ \bar{w}e_{\sigma^{[i]}-1}, & \sigma^{[i]} = 5, 6, 7 \\ -\bar{v}e_{\sigma^{[i]}-7}, & \sigma^{[i]} = 8, 9, 10 \\ -\bar{w}e_{\sigma^{[i]}-7}, & \sigma^{[i]} = 11, 12, 13 \end{cases}. \quad (3)$$

Here, \bar{v} and \bar{w} are predefined velocities, and $e_{(\cdot)}$ denotes the canonical basis of \mathbb{R}^6 . The continuous-time switched model for UAV i becomes:

$$\dot{x}^{[i]} = f_{\sigma^{[i]}}(x^{[i]}, u^{[i]}(\sigma^{[i]})), \quad x^{[i]}(0) = x_0^{[i]}. \quad (4)$$

For implementation, we use the discrete version with sampling time $T > 0$ and the integer k as sampling instant given by

$$\begin{aligned} x_{k+1}^{[i]} &= x_k^{[i]} + T f_{\sigma_k}^{[i]}(x_k^{[i]}, u_k^{[i]}(\sigma_k^{[i]})), \\ x_{k+1}^{[i]} &= f_{d\sigma_k}(x_k^{[i]}, u_k^{[i]}(\sigma_k^{[i]})). \end{aligned} \quad (5)$$

2.3 Problem statement

Consider a closed 3D environment with N_r identical quadrotor UAVs governed by (5), each equipped with localization sensors, and N_{obs} uncontrolled moving obstacles. The objective is to design a distributed switched predictive control strategy that autonomously guides each UAV to its reference position while ensuring collision avoidance with both obstacles and fellow agents.

3. MAIN RESULTS

Managing multi-agent systems becomes computationally demanding as the number of subsystems increases, especially under centralized coordination. Therefore, to address this, we adopt a distributed communication scheme that distributes the computational load among agents.

Following the sequential distributed strategy in (Christofides et al., 2013), each UAV locally solves an SMPC using a cluster-based topology. Spherical clusters with radius r_{cl} are centered at each UAV's reference position, and agents

within the same cluster are considered neighbors. The cluster membership for UAV i at time k is defined by:

$$\mathcal{C}_k^{[i]} := \{j \in \mathcal{N} \mid \|p_k^{[i]} - p_k^{[j]}\|_2 < r_{\text{cl}}, j \neq i\}. \quad (6)$$

Letting N be the horizon length, associated state and input information for the agents in $\mathcal{C}_k^{[i]}$ are collected in:

$$\begin{aligned} \mathcal{X}_{\mathcal{C}_k}^{[i]} &:= \{x_k^{[j]} \in \mathbb{R}^6 \mid j \in \mathcal{C}_k^{[i]}\}, \\ \mathcal{U}_{\mathcal{C}_k}^{[i]} &:= \{\mathbf{u}_k^{[j]} = [\hat{u}_{k+1}^{[j]}, \dots, \hat{u}_{k+N-1}^{[j]}] \mid j \in \mathcal{C}_k^{[i]}\}. \end{aligned} \quad (7)$$

To enhance robustness, we share only the optimal predicted input sequence $\mathcal{U}_{\mathcal{C}_k}^{[i]}$ instead of full predicted trajectories, avoiding noise propagation from state measurements.

In this sequential setup, agents solve their SMPCs in a predefined order, each using updated input data from previously solved neighbors. At $k = 0$, $\mathcal{U}_{\mathcal{C}_k}^{[i]}$ is empty; this is addressed either by initializing $\mathcal{C}_k^{[i]} = \emptyset$ or assuming neighbors remain static (Huancá et al., 2023). This procedure is recursively applied to all agents yet to solve their optimal control problems. Fig. 1 illustrates this distributed framework, showing subsystem clusters and inter-agent communication links.

3.1 Koopman operator-based collision avoidance

Collision avoidance is essential for UAVs, particularly in environments with dynamic and unknown obstacles. This work addresses such challenges by predicting obstacle trajectories using the Koopman operator, which transforms nonlinear dynamics into a linear framework through lifted observables. For a nonlinear discrete-time system $z(k+1) = f(z(k))$, with state $z(k) \in \mathbb{R}^n$, the Koopman operator \mathcal{K} governs the evolution of observables $g(z)$ via

$$g(z(k+1)) = \mathcal{K}g(z(k)). \quad (8)$$

In the following, for the sake of simplicity, we adopt the notation $g_k(z_k)$ standing for $g(z(k))$. This enables linear prediction of complex dynamics using data-driven approximations (Williams et al., 2015; Zhang et al., 2019). Let $o_k^{[l_o]} \in \mathbb{R}^3$ be the estimated position of the l_o -th obstacle at time k . During each open-loop iteration, the lifted prediction evolves as (Bueno et al., 2025):

$$g_{t+1}(o_{t+1}^{[l_o]}) = \mathcal{K}g_t(o_t^{[l_o]}), \quad \forall t \in \mathcal{T}_k, \quad (9)$$

with $\mathcal{T}_k = \{k, \dots, k+N-1\}$, with $N > 0$ being the prediction horizon. The predicted position $o_t^{[l_o]}$ is extracted from $g_t(o_t^{[l_o]})$. These predicted positions are modeled as spherical obstacles. The collision constraint between UAV i and obstacle l_o is:

$$\|p_t^{[i]} - o_t^{[l_o]}\|_2 \geq R^{[i]} + R^{[l_o]} + \delta^{[i, l_o]}, \quad (10)$$

where $R^{[i]}$ and $R^{[l_o]}$ denote safety radii, and $\delta^{[l_o]}$ is a safety margin. Due to its nonlinearity, we approximate the sphere by a polytope defined by $\gamma_t^{[i, l_o]}$ linear inequalities, i.e.,

$$(\eta_{t, \mu}^{[i, l_o]})^\top (p_t^{[i]} - o_t^{[l_o]}) \leq d_t^{[i, l_o]}, \quad \mu = 1, \dots, \gamma_t^{[i, l_o]}, \quad (11)$$

with $\eta_{t, \mu}^{[i, l_o]}$ as normal vectors and $d_t^{[i, l_o]}$ the corresponding plane distances. To enforce the safe distance, we compute the signed distances as

$$\rho_{t, \mu}^{[i, l_o]} = (\eta_{t, \mu}^{[i, l_o]})^\top (p_t^{[i]} - o_t^{[l_o]}) - d_t^{[i, l_o]}, \quad (12)$$

and select the most restrictive plane with

$$\mu_{t, \max}^{[i, l_o]} = \arg \max_{\mu} \rho_{t, \mu}^{[i, l_o]}. \quad (13)$$

The linear constraint ensuring avoidance becomes

$$(\eta_{t, \mu_{t, \max}^{[i, l_o]}}^{[i, l_o]})^\top (p_t^{[i]} - o_t^{[l_o]}) \geq d_t^{[i, l_o]}. \quad (14)$$

For inter-agent avoidance, a similar constraint applies, i.e.,

$$\|p_t^{[i]} - p_t^{[j]}\|_2 \geq R^{[i]} + R^{[j]} + \delta^{[i, j]}, \quad (15)$$

leading to the linearized version given by

$$(\eta_{t, \mu_{t, \max}^{[i, j]}}^{[i, j]})^\top (p_t^{[i]} - p_t^{[j]}) \geq d_t^{[i, j]}. \quad (16)$$

These linear constraints ensure computational tractability and effective avoidance of both dynamic obstacles and other agents.

3.2 Finite horizon optimal control problem

Considering (3), (5), and linearized constraints (14) and (16), the optimal control problem for the i -th UAV is formulated as:

$$\min_{\sigma_k^{[i]}} \sum_{t \in \mathcal{T}_k} \|p_t^{[i]} - p_{\text{ref}}^{[i]}\|_2, \quad (17a)$$

$$\text{s.t. } \forall t \in \mathcal{T}_k, j \in \mathcal{C}_k^{[i]}, j \neq i, l = 1, \dots, N_{\text{obs}}, \\ x_{t+1}^{[i]} = f_{\sigma_t^{[i]}}^{\text{d}}(x_t^{[i]}, u_t^{[i]}(\sigma_t^{[i]})), \quad x_k^{[i]} = \tilde{x}_k^{[i]}, \quad (17b)$$

$$u_t^{[i]} \in \mathcal{U}_{\text{sw}}, \quad (17c)$$

$$(\eta_{t, \mu_{t, \max}^{[i, l_o]}}^{[i, l_o]})^\top (p_t^{[i]} - o_t^{[l_o]}) \geq d_t^{[i, l_o]}, \quad (17d)$$

$$(\eta_{t, \mu_{t, \max}^{[i, j]}}^{[i, j]})^\top (p_t^{[i]} - p_t^{[j]}) \geq d_t^{[i, j]}. \quad (17e)$$

Here, $\tilde{x}_k^{[i]}$ denotes the current state measurement. The cost (17a) penalizes deviation from the reference position $p_{\text{ref}}^{[i]}$ across the prediction horizon N . The Koopman-based obstacle prediction informs constraint (17d), while inter-agent safety is enforced through (17e).

4. SIMULATION RESULTS

The simulation results are presented in two parts to highlight the effectiveness of the proposed Koopman-based modeling and prediction, as well as its integration with the SMPC framework for dynamic obstacle avoidance.

4.1 Koopman-based prediction of moving objects

In the first scenario, $N_r = 3$ UAVs monitor a ground-moving obstacle without executing the SMPC task, emphasizing the Koopman-based approach's ability to model and predict unknown dynamics over time. Sensor noise is applied based on the UAV-obstacle distance, realistically simulating measurement accuracy degradation with range. Once an obstacle enters the sensor range, it is continuously tracked, and position measurements are stored in a finite buffer. Upon collecting enough data, the Koopman operator \mathcal{K} is computed (Bueno et al., 2025), yielding a linear approximation of the obstacle's behavior. To represent the motion, the lifting function is defined as:

$$g(o^{[l_o]}) = [g(o_x^{[l_o]})^\top, g(o_y^{[l_o]})^\top]^\top,$$

$$g(o_\zeta^{[l_o]}) = [\zeta, \zeta^2, \sin(\zeta), \cos(\zeta), \zeta^2 \sin(\zeta), \zeta^2 \cos(\zeta)]^\top,$$

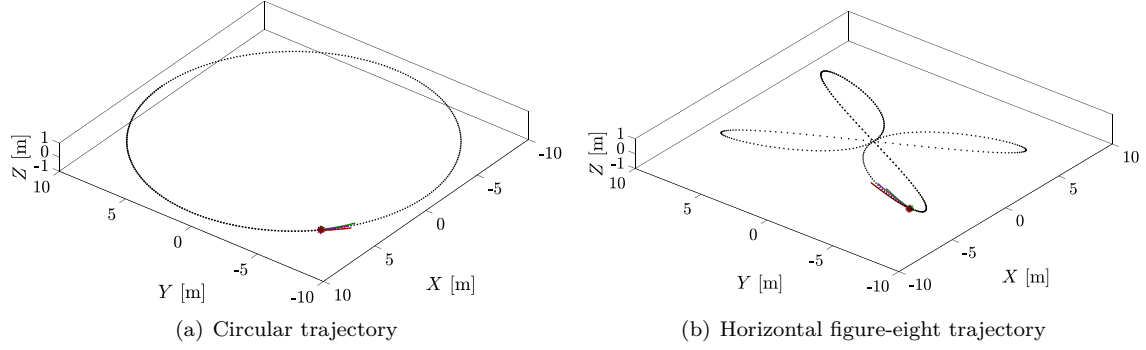


Fig. 2. Tracking and prediction of moving obstacles.

Table 1. Prediction error comparison.

Motion Type	Nonlinear GP (Olcay et al., 2024)			Koopman (Proposed)		
	RMSE	MAE	MaxErr	RMSE	MAE	MaxErr
Circular ($X - Y$ plane)	64.2611	56.6285	110.9384	51.6039	48.4821	77.0244
Planar Figure-Eight Trajectory ($X - Y$ plane)	83.4153	72.8220	146.1566	69.2424	63.4870	108.2167
3-dimensional Butterfly Curve	78.1790	68.8219	135.4376	39.5392	37.3492	53.0990

where $\zeta \in \{x^{[l_o]}, y^{[l_o]}\}$ are the measured positions of the l_o -th obstacle. This formulation captures diverse dynamics by incorporating polynomial and trigonometric interactions, enabling the modeling of both smooth and complex nonlinear behaviors. Two distinct obstacle motions are considered: a circular trajectory in the $X - Y$ plane and a horizontal figure-eight path. The former reflects structured periodic motion typical in surveillance or patrol tasks, while the latter introduces variable curvature and speed, representing more complex adaptive behaviors. These trajectories offer a realistic benchmark for evaluating prediction performance in dynamic environments. Using the most recent observation, the Koopman model iteratively forecasts future positions over a finite horizon. As shown in Fig. 2 for a specific sample time, predicted trajectories (solid lines) closely follow the actual path (dotted line), even with distance-dependent measurement noise. This highlights the Koopman approach's robustness and its utility in enabling proactive, collision-free path planning in the full control scenario.

4.2 Comparison and discussion

To validate the proposed obstacle prediction approach, we evaluate three standard metrics: root mean square error (RMSE), mean absolute error (MAE), and maximum

absolute error (MaxErr). The Koopman-based method is compared against the nonlinear Gaussian process (GP) regression approach from (Olcay et al., 2024), which employs a custom basis function and a squared exponential kernel. Table 1 summarizes the accumulated prediction errors computed over time by the three UAVs predicting obstacle motion online across three motion patterns. In all cases, the Koopman model outperforms the GP-based approach. For circular motion, RMSE drops from 64.26 to 51.60 and MaxErr from 110.94 to 77.02. In the planar figure-eight case, RMSE decreases from 83.41 to 69.24, with notable MAE and MaxErr improvements. The most significant gains appear in the 3-dimensional butterfly trajectory, where RMSE and MaxErr reduce from 78.18 and 135.44 to 39.54 and 53.10, respectively. These results demonstrate the Koopman model's superior generalization and robustness in nonlinear motion prediction.

4.3 SMPC with dynamic obstacle avoidance

In the second scenario, UAVs perform obstacle avoidance using the SMPC framework while leveraging the Koopman-based predictions. The simulation uses a sampling time $T = 0.01$ s and horizon $N = 4$, over a 35-second window. UAVs and obstacles share the same physical parameters, including a frame radius $r_{\text{rob}} = r_{\text{obs}} = 0.1125$ m, used to define encapsulating spheres and tuning parameters. A team of $N_r = 4$ controllable UAVs with dynamics (5) and predefined velocities $\bar{v} = 0.2$ m.s⁻¹, $\bar{w} = 0.6$ rad.s⁻¹ begins at

$$x^{[i]}(0) = r_{\text{init}} \left[\cos \frac{2\pi(i-1)}{N_r}, \sin \frac{2\pi(i-1)}{N_r}, \mathbf{0}_4^\top \right]^\top, \quad (18)$$

with $r_{\text{init}} = 3.5$ m and $i = 1, \dots, N_r$. Communication is allowed within clusters of radius $r_{\text{cl}} = 8r_{\text{rob}}$. We deploy $N_{\text{obs}} = 8$ uncontrolled obstacles arranged in two groups. Each obstacle's position is given by

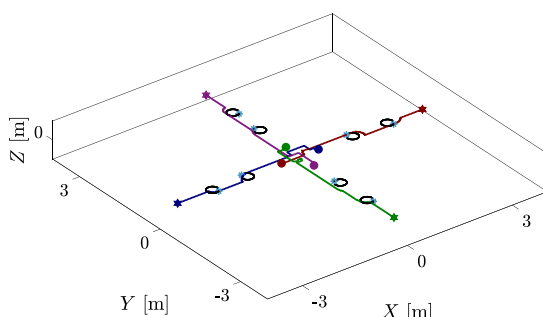


Fig. 3. Ultimate positions of obstacles and UAVs as well as their trajectories over time.

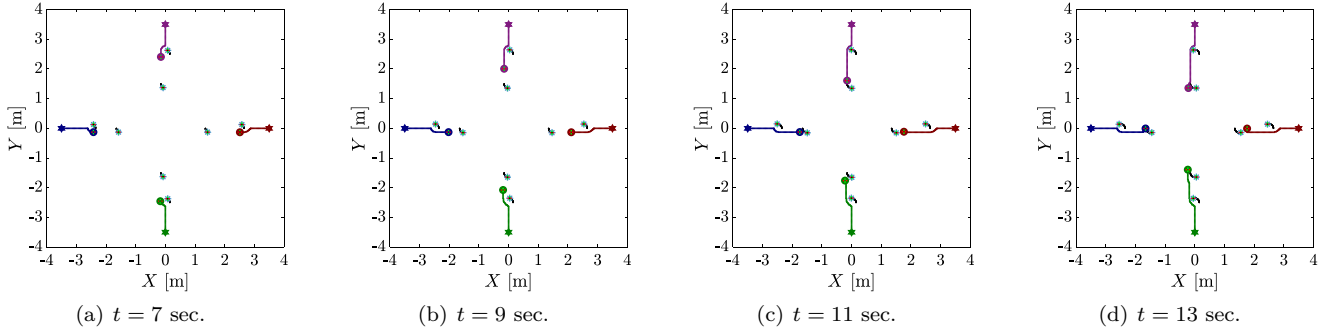


Fig. 4. Snapshots of UAVs and obstacles positions at different time instances.

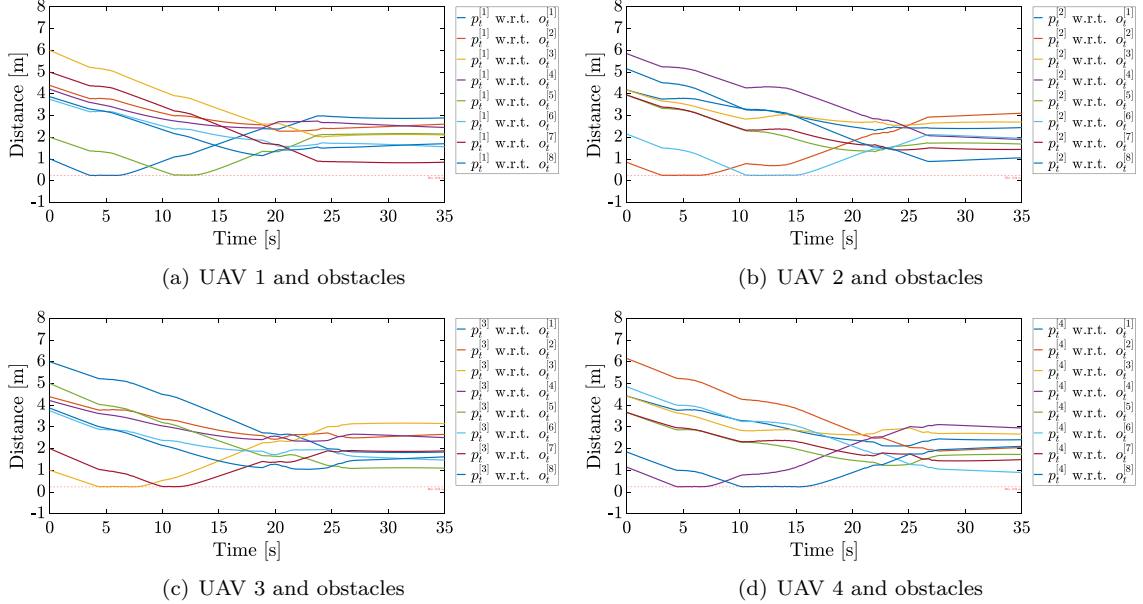


Fig. 5. Evolution of Euclidean UAV-to-obstacle distances. Highlighted minima for safe separation is 0.24 m.

$$\begin{aligned} x_{\text{ring}}^{[l,q]} &= r_{\text{ring}}^{[q]} \left[\cos \frac{4\pi(l-1)}{N_{\text{obs}}}, \sin \frac{4\pi(l-1)}{N_{\text{obs}}}, 0 \right]^\top, \\ x_{\text{cov}}^{[l,q]} &= r_{\text{cov}}^{[q]} \left[\cos \alpha_t^{[l,q]}, \sin \alpha_t^{[l,q]}, 0 \right]^\top, \\ x_{\text{obs}}^{[l,q]} &= x_{\text{ring}}^{[l,q]} + x_{\text{cov}}^{[l,q]}, \end{aligned} \quad (19)$$

where $l = 1, \dots, 4$ is the index of obstacles inside a q -th ring, $q = 1, 2$, with ring radii equal to $r_{\text{ring}}^{[1]} = 2.5$ m, $r_{\text{ring}}^{[2]} = 1.5$ m, $r_{\text{cov}} = 0.3$ m is the radius of the covered path, and $\alpha_t^{[l,q]}$ is the angular position of the obstacle along the covered path, with angular velocity chosen as 0.15 rad/s. The reference positions lie at the vertices of a square

centered at the origin, i.e.,

$$x_{\text{ref}}^{[i]} = r_{\text{ref}} \left[-\cos \frac{2\pi(i-1)}{N_r}, -\sin \frac{2\pi(i-1)}{N_r}, \mathbf{0}_4^\top \right]^\top, \quad (20)$$

with $r_{\text{ref}} = 0.5$ m and $i = 1, \dots, N_r$.

Since UAVs are actively navigating, obstacle center of mass positions are measured by fixed ceiling cameras and relayed in real time. In the simulation all motion occurs in the $X - Y$ plane, avoiding Z -direction maneuvers, thus enforcing challenging coordinated responses to dynamic obstacles which are constrained to the 2-dimensional domain. This setup highlights the true capability of the Koopman-based prediction and switching control strategy.

Fig. 3 shows UAV trajectories navigating a dynamic environment with moving obstacles, culminating in successful formation while avoiding collisions. The Koopman-based prediction integrated with SMPC enables real-time, coordinated, and safe navigation to the target configuration. To further illustrate system behavior, Fig. 4 provides snapshots at selected time steps, showing UAV positions relative to obstacles. These frames reveal how agents dynamically adjust paths to avoid collisions while maintaining formation. Safety is assessed in Figs. 5(a)-5(d) and Fig. 6, which display UAV-obstacle and inter-agent distances over time, with minimum distances highlighted. All separations remain

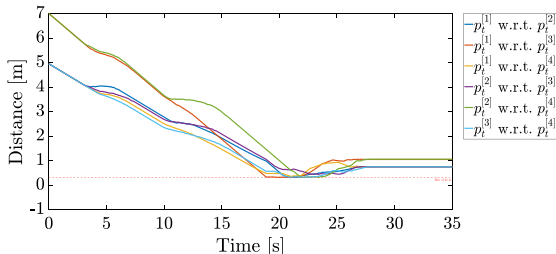


Fig. 6. Evolution of Euclidean inter-agent distances. Highlighted minima is 0.31 [m].

above twice the UAV radius, confirming collision-free operation. This validates the effectiveness of our Koopman-SMPC framework in maintaining safety margins during navigation.

5. CONCLUSIONS

This paper introduced a Koopman-integrated distributed SMPC framework for cooperative UAV navigation in dynamic environments. The switching-based control reduces computation while retaining responsive planning. Leveraging the Koopman operator enables efficient prediction of obstacles prediction. The distributed design enhances scalability and autonomy, supporting UAV traffic management. Simulations validate safe, collision-free navigation with preserved formation, showing promising results for aerial and surface mobility. Future works include extending to heterogeneous agents, aerial-ground coordination, and learning-based switching for dynamic environments.

REFERENCES

Bemporad, A. and Morari, M. (1999). Control of systems integrating logic, dynamics, and constraints. *Automatica*, 35(3), 407–427.

Bueno, V., Azarbahram, A., Farina, M., and Fagiano, L. (2025). Koopman-based dynamic environment prediction for safe uav navigation. *arXiv preprint arXiv:2511.06990*.

Christofides, P.D., Scattolini, R., Muñoz de la Peña, D., and Liu, J. (2013). Distributed model predictive control: A tutorial review and future research directions. *Computers & Chemical Engineering*, 51, 21–41. CPC VIII.

Comas, A., Ghimire, S., Li, H., Sznaier, M., and Camps, O. (2021). Self-supervised decomposition, disentanglement and prediction of video sequences while interpreting dynamics: A koopman perspective. *arXiv preprint arXiv:2110.00547*.

Garcia, C.E., Prett, D.M., and Morari, M. (1989). Model predictive control: Theory and practice—a survey. *Automatica*, 25(3), 335–348.

Gutow, G. and Rogers, J.D. (2020). Koopman operator method for chance-constrained motion primitive planning. *IEEE Robotics and Automation Letters*, 5(2), 1572–1578.

Hrabar, S. (2011). Reactive obstacle avoidance for rotorcraft uavs. In *2011 IEEE/RSJ International Conference on Intelligent Robots and Systems*, 4967–4974. IEEE.

Huanca, C.P.E.Y., Incremona, G.P., and Colaneri, P. (2023). Design of a distributed switching model predictive control for quadrotor uavs aggregation. *IEEE Control Systems Letters*, 7, 2964–2969.

Korda, M. and Mezić, I. (2018). Linear predictors for nonlinear dynamical systems: Koopman operator meets model predictive control. *Automatica*, 93, 149–160.

Kouvaritakis, B. and Cannon, M. (2016). Model predictive control. *Switzerland: Springer International Publishing*, 38, 13–56.

Li, M., Sun, Z., Liao, Z., and Weiland, S. (2023). Moving obstacle collision avoidance via chance-constrained mpc with cbf. *arXiv preprint arXiv:2304.01639*.

Liu, S., Watterson, M., Mohta, K., Sun, K., Bhattacharya, S., Taylor, C.J., and Kumar, V. (2017). Planning dynamically feasible trajectories for quadrotors using safe flight corridors in 3-d complex environments. *IEEE Robotics and Automation Letters*, 2(3), 1688–1695.

Manzoor, W.A., Rawashdeh, S., and Mohammadi, A. (2023). Vehicular applications of koopman operator theory—a survey. *IEEE Access*, 11, 25917–25931.

Mauroy, A., Susuki, Y., and Mezic, I. (2020). *Koopman operator in systems and control*, volume 7. Springer.

Mayne, D.Q., Seron, M.M., and Raković, S.V. (2005). Robust model predictive control of constrained linear systems with bounded disturbances. *Automatica*, 41(2), 219–224.

Mezić, I. (2021). Koopman operator, geometry, and learning of dynamical systems. *Not. Am. Math. Soc.*, 68(7), 1087–1105.

Michael, N., Fink, J., and Kumar, V. (2011). Cooperative manipulation and transportation with aerial robots. *Autonomous Robots*, 30, 73–86.

Olcay, E., Meeß, H., and Elger, G. (2024). Dynamic obstacle avoidance for uavs using mpc and gp-based motion forecast. In *2024 European Control Conference (ECC)*, 1024–1031. IEEE.

Oleynikova, H., Burri, M., Taylor, Z., Nieto, J., Siegwart, R., and Galceran, E. (2016). Continuous-time trajectory optimization for online uav replanning. In *2016 IEEE/RSJ International Conference on Intelligent Robots and Systems (IROS)*, 5332–5339.

Ponda, S., Redding, J., Choi, H.L., How, J.P., Vavrina, M., and Vian, J. (2010). Decentralized planning for complex missions with dynamic communication constraints. In *Proceedings of the 2010 American Control Conference*, 3998–4003. IEEE.

Saccani, D., Cecchin, L., and Fagiano, L. (2022). Multitrajectory model predictive control for safe uav navigation in an unknown environment. *IEEE Transactions on Control Systems Technology*, 31(5), 1982–1997.

Scherer, S., Singh, S., Chamberlain, L., and Elgersma, M. (2008). Flying fast and low among obstacles: Methodology and experiments. *The International Journal of Robotics Research*, 27(5), 549–574.

Tang, S. and Kumar, V. (2018). Autonomous flight. *Annual Review of Control, Robotics, and Autonomous Systems*, 1(1), 29–52.

Wei, S.X., Dixit, A., Tomar, S., and Burdick, J.W. (2022). Moving obstacle avoidance: A data-driven risk-aware approach. *IEEE Control Systems Letters*, 7, 289–294.

Williams, M.O., Kevrekidis, I.G., and Rowley, C.W. (2015). A data-driven approximation of the koopman operator: Extending dynamic mode decomposition. *Journal of Nonlinear Science*, 25, 1307–1346.

Zhang, H., Rowley, C.W., Deem, E.A., and Cattafesta, L.N. (2019). Online dynamic mode decomposition for time-varying systems. *SIAM Journal on Applied Dynamical Systems*, 18(3), 1586–1609.

Zhang, X., Pan, W., Scattolini, R., Yu, S., and Xu, X. (2022). Robust tube-based model predictive control with koopman operators. *Automatica*, 137, 110114.

Zhou, D. and Schwager, M. (2015). Virtual rigid bodies for coordinated agile maneuvering of teams of micro aerial vehicles. In *2015 IEEE International Conference on Robotics and Automation (ICRA)*, 1737–1742. IEEE.